

An innovative approach for the fabrication of highly conductive nanocomposites with different carbon

Henry Kuo Feng Cheng^{1,2}, Nanda Gopal Sahoo¹, Lin Li¹, Siew Hwa Chan¹, Jianhong Zhao²

¹ School of Mechanical and Aerospace Engineering, Nanyang Technological University, 50 Nanyang Avenue, Singapore 639798

² Singapore Institute of Manufacturing Technology, 71 Nanyang Drive, Singapore 638075

Abstract. A novel approach to the preparation of a super-conductive polymeric nanocomposite system with different carbon fillers is presented. The ternary composites of polyamide 6 (PA6) and conductive carbon black (CCB) and multi-walled carbon nanotubes (MWCNTs) were fabricated by a melt-mixing technique. The ternary nanocomposites with the high filler contents showed extremely higher conductivity compared with the corresponding binary polymer composites. The effects of CCB and MWCNTs at different compositions on the rheological, physical, morphological, thermal, mechanical, and electrical properties of the ternary nanocomposites have been studied systematically. A mechanism for the complementary effects of CCB and MWCNTs has been proposed.

Keywords: carbon black, carbon nanotube, electrical conductivity, nanocomposites, polyamides

1. Introduction

Carbon black (CB) is a material that has been widely used for many years as a reinforcing agent. Especially in the tyre industry, carbon black has been used in rubber as a reinforcing filler to improve mechanical properties.^[1, 2] Polymer-carbon black composites have higher electrical properties^[3-8] and higher strengths^[9-11] than those of their pure polymeric matrices. Nowadays, a special type of CB, conductive carbon black (CCB),^[8] is available and is added into polymers in order to achieve improvements in the thermal and electrical properties of polymers.

Carbon nanotubes (CNTs), since being first reported,^[12] are the most attractive fillers for polymer nanocomposites with superior properties. This is because of their unique properties and structure.^[13-16] However, due to their high surface energy, high aspect ratio and strong van der Waals force, CNTs have a great tendency to form agglomerates and this is the greatest challenge for the development of high performance polymer composites by uniformly dispersing CNTs into the polymers. Among the methods used to overcome this agglomeration problem, melt mixing is compatible with

current industrial practices. In this process, CNTs are mechanically dispersed into a polymer melt using a high shear force compounder.^[17]

From the literature,^[18-26] we know that it is very difficult to produce a polymer composite with a very high conductivity by adding a single type of filler such as CNTs or CCBs alone. In this study, we, therefore, are particularly interested in the fabrication of highly conductive polymer composites filled with both CNTs and CCB. In our approach to advanced conductive polymer composites, both multi-walled carbon nanotubes (MWCNTs) and conductive carbon black (CCB) were added into a polyamide6 (PA6) matrix. The effects of both MWCNTs and CCB in different compositions on the rheological, morphological and electrical properties of the PA6/CCB/MWCNT ternary composites have been examined. A complementary effect has surprisingly been found between MWCNTs and CCB in the polymer matrix, which endows the ternary composites with superior electrical and thermal properties.

2. Experimental work

2.1 Materials and sample preparation

Polyamide 6 (PA6) (Ultrad B36 LN 01) was purchased from BASF. The conductive carbon black (CCB, ENSACO 350G) was supplied by Timcal. The properties of CCB supplied by the manufacturer were the density (135 kg/m³), particles size (45.0 nm), and volume resistivity (< 20.0 Ω-cm), respectively. The multi-walled carbon nanotubes (MWCNTs, Baytubes® C 150 HP) were purchased from Bayer Material Science. According to the manufacturer, the diameter, length, number of walls and bulk density were 5 - 20 nm, 1 ~ > 10 μm, 3 - 15 and 140 - 230 kg/m³, respectively.

Prior to mixing, the PA6, CCB and MWCNTs were dried at 60 °C for 12 hrs in a vacuum oven. Compounding for PA6/MWCNT, PA6/CCB and PA6/CCB/MWCNT composites was carried out in a HAAKE PolyLab, an internal mixer, equipped with two counter-rotating screws at 300°C and at a mixing speed of 30 rpm for 15 min. After being taken out from the mixer, the composites were molded into different shapes at 300 °C and an injection pressure of 60 MPa using a HAAKE MiniJet, a mini injection machine. The formulations and sample codes are tabulated in Table 1.

Table 1. The sample codes and formulations for the composites (in weight percentage)

| Code | PA6 | PB10 | PN10 | PB20 | PN20 | PBN10 |
|------|-----|------|------|------|------|-------|
| PA6 | 100 | 90 | 90 | 80 | 80 | 80 |
| CCB | - | 10 | - | 20 | - | 10 |
| CNT | - | - | 10 | - | 20 | 10 |

2.2 Measurements

The rheological measurements were performed on a rotational rheometer (Anton Paar – Physica MCR301) with the samples of $\Phi 25$ mm x 1 mm. The experiments were carried out in a frequency sweep mode at 5% constant strain using parallel plates with a diameter of 25 mm at 300°C in dry nitrogen.

The surface morphology of the fractured samples was observed by scanning electron microscopy (SEM), after silver coating. The analysis was done using a JEOL JSM-5800 SEM.

Direct Current (DC) electrical conductivity measurements were carried out at room temperature using a probe station of four-pointed fixture (CASCADE – REL 4800) combined with a precision LCR meter (HP Agilent – 4284A). The applied voltage was varied from 0.01 to 1.00 V.

3. Results and Discussion

3.1 Effects of CCB and MWCNTs on rheological properties of PA6

Dynamic frequency sweep tests were used to explore the structure and network formation of the composites. The changes in complex viscosity (η^*) with respect to angular frequency for the pure PA6, the PA6/CCB, PA6/MWCNT and PA6/CCB/MWCNT composites at 300 °C are shown in Figure 1. The power law index for complex viscosity varies with the loading of carbon filler; details are listed in Table 2.

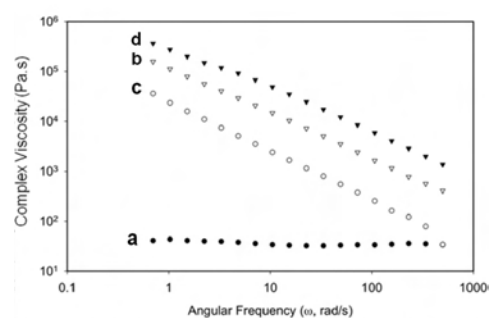


Fig. 1. Complex viscosity versus angular frequency for pure PA6, PBN, PB and PN composites at 300 °C, where: (a) PA6, (b) PBN10, (c) PB20 and (d) PN20.

Table 2. Power law index of complex viscosity, the slope of G' and G'' with respect to angular frequency for PB, PN, and PBN composites

| Sample Code | Power law index of $\log \eta^*$ Vs $\log \omega$ | Slope of $\log G'$ Vs $\log \omega$ | Slope of $\log G''$ Vs $\log \omega$ |
|-------------|---|-------------------------------------|--------------------------------------|
| PA6 | 0.03 | 1.572 | 0.958 |
| PBN10 | 0.93 | 0.103 | 0.013 |
| PB20 | 1.00 | 0.027 | 0.00 |
| PN20 | 0.85 | 0.221 | 0.01 |

Over the range of angular frequency applied, the power law index for complex viscosity, η^* , increased with increasing carbon loading from $\omega^{0.03}$ for pure PA6 to $\omega^{0.93}$ for PBN10, $\omega^{1.00}$ for PB20 and $\omega^{0.85}$ for PN20. The power law index for pure PA6 is 0.03, which tells that the flow is almost a Newtonian one but the power law index increases as the carbon loading increase. These increases in power law show the flow behaviour changes from Newtonian to non-Newtonian. As was expected, the viscosities of the composites gradually increased with increasing carbon content which could be concluded to result from the formation of a dense MWCNT-CCB network in the polymer, as shown in Fig 1. From this figure, compared to the CCB-alone composite (PB20), the ternary composite (PBN10) has a higher viscosity but the viscosity of PBN10 is lower than that of the MWCNT-alone composite (PN20). This is probably due to MWCNT with a high aspect ratio could restrict the flow of the polymer chains in their molten state, while CCB with a spherical structure (in its powder-form) could have less effect. As a result, the mixture of the high aspect ratio MWCNT and spherical CCB results in the intermediate viscosity of ternary composites. On the other hand, the higher viscosity of MWCNT-alone composites increases the difficulty in dispersing MWCNTs into the polymer matrix, thus leading to a relative worse

dispersion than CCB in CCB-alone composites as is discussed in the following sections.

Similarly, addition of MWCNTs and CCB influences the frequency-dependence of the storage modulus (G') and loss modulus (G''), especially at low frequencies. Storage modulus and loss modulus versus angular frequency for pure PA6, PA6/CCB, PA6/MWCNT and PA6/CCB/MWCNT composites at 300 °C are shown in Figures 2 and 3, respectively. Over the range of angular frequency applied, pure PA6 tended to exhibit a typical terminal flow behaviour with the scaling properties of $G' \approx \omega^2$ and $G'' \approx \omega^1$ as ω was approaching 0 in accordance with the theory of linear viscoelasticity.^[27] But for all the composite samples, the dependence of G' on ω became smaller with increasing carbon loading. Thus, polymer chain relaxation in the composites was effectively controlled by the presence of carbon fillers. The decreases in the power law index, which is related to the dependency of G' on ω , with the loading of carbon fillers, are listed in Table 2.

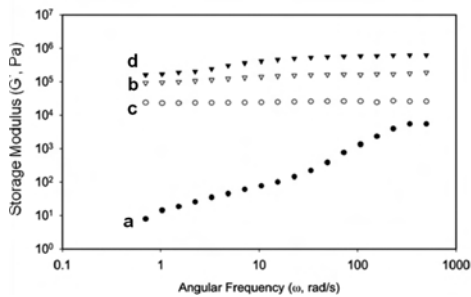


Fig. 2. Storage modulus versus angular frequency for pure PA6, PBN, PB and PN composites at 300 °C, where: (a) PA6, (b) PBN10, (c) PB20 and (d) PN20.

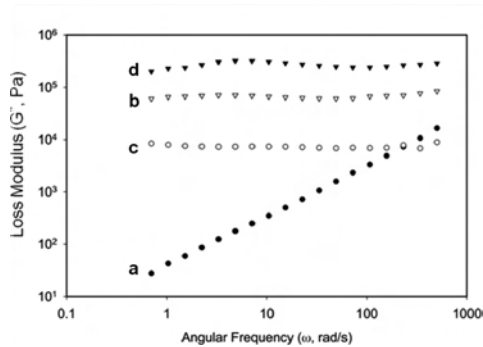


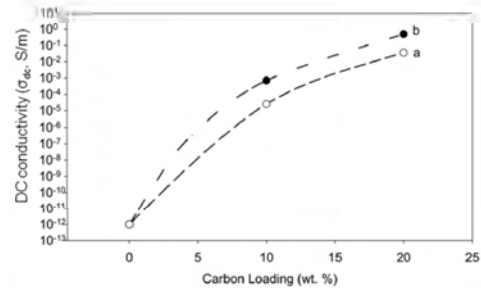
Fig. 3. Loss modulus versus angular frequency for pure PA6, PBN, PB and PN composites at 300 °C, where: (a) PA6, (b) PBN10, (c) PB20 and (d) PN20

The power law index for G' decreased with increase carbon loading from $\omega^{1.572}$ for pure PA6 to $\omega^{0.103}$ for PBN10, $\omega^{0.027}$ for PB20 and $\omega^{0.221}$ for PN20, respectively. The loss moduli of the composites exhibited a similar trend to the storage moduli. The frequency dependency of G'' also decreased from $\omega^{0.958}$ for pure PA6 to $\omega^{0.013}$ for

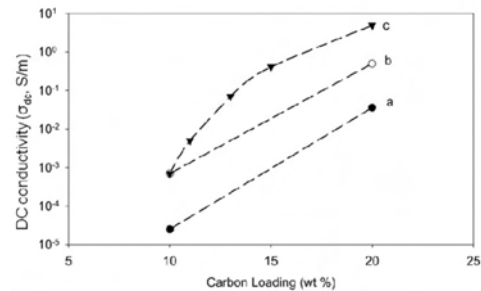
PBN10, $\omega^{0.001}$ for PB20, and $\omega^{0.01}$ for PN20, respectively. These decreases in the power law index of G' and G'' indicated a transitional behavior from a liquid-like to a solid-like viscoelastic flow. This phenomenon is mainly related to interactions between particles and network formation as the inter-particle distance decreases. This network significantly influenced not only rheological properties but also electrical ones of the composites, which is discussed in the following sections.

3.2 Electrical conductivity of PA6 induced by CCB and MWCNT

The comparison of DC electrical conductivity between PA6/CCB (PB) composites and PA6/MWCNT (PN) composites is as shown in Figure 4A. From this figure, PB20 has a conductivity of 0.5 S/m while PN20 has that of 0.04 S/m. So, it can be concluded that the composites with CCB alone have higher DC conductivity than those with MWCNTs alone although electrical conductivity of MWCNTs is higher than that of CCB.



(A)



(B)

Fig. 4. DC electrical conductivities for (a) PN composites, (b) PB composites and (c) PBN composites at different carbon loadings.

Surprisingly, when MWCNTs were added into the PA6 composite with 10 wt.-% CCB to make the ternary composites, there was another percolation leading to a significant improvement in the electrical conductivity of the resulting ternary composites. The comparison of conductivity among the three different composite systems is as shown in Figure 4B. The conductivity of the ternary composite (PBN5) is 0.4 S/m, which is 80 % of that of PB20 (0.5 S/m). This is 10 times higher than that of PN20

(0.04 S/m). At 20 wt.-% of carbon loading, the PBN10 (5 S/m) (the ternary composite with PA6, 10 wt.-% CCB and 10 wt.-% MWCNT) showed about 10 times higher in conductivity than PB20 (0.5 S/m) (the binary composite with PA6 and 20 wt.-% CCB) and about 125 times higher in conductivity than PN20 (0.04 S/m) (the binary composite with PA6 and 20 wt.-% MWCNT).

3.3 Enhanced electrical conductivity due to the formation of a conductive network from MWCNTs and CCB

CCB has the high surface energy and the relatively high conductivity while MWCNTs exhibit the high aspect ratio and excellent conductivity. Therefore, both CCBs and MWCNTs are outstanding candidates for the fabrication of conducting polymer composites. Figure 5 shows the FESEM micrographs of PN, PB and PBN composites. Referring to circles in Figure 5a, due to the agglomeration of MWCNTs resulting from the strong van der Waals forces of MWCNTs and high viscosity of MWCNT composite during the compounding process, MWCNT-based composites have a major drawback in conducting electricity. On the other hand, due to the inherent properties of CCB,^[8] it is possible for it to form a spider-like 3D network in the polymer matrix indicated by circles in Figure 5b. Then, according to Figure 5c, in the ternary composites of PA6, CCB and MWCNTs, CCB still can maintain its spider-like 3D structure (denoted by the circle A) while there are some MWCNT agglomerates (indicated by the circle B) in the composites. Moreover, there is interestingly observed a connection between the CCB network and MWCNT agglomerates (denoted by the circle C), which makes the network of the ternary composites more perfect and as a result, they have higher electrical conductivities.

According to Figure 4, it has been proved that the ternary composites have better conductivities than the binary composites. From these results, a possible mechanism explaining why the electrical conductivity of ternary composites is higher than that of their correspondent binary composites, is proposed in Figure 6. This proposed figure is an analytical sketch based on the FESEM micrographs from Figure 5. Although MWCNTs exhibit the high aspect ratio and high conductivity, MWCNTs tend to agglomerate themselves due to their strong van der Waals force and they are present as bundles in the polymer matrix as shown in Figure 5a (denoted by the circles). Therefore, we can conclude that it is extremely difficult for MWCNTs to form a conductive network as illustrated in Figure 6a. As a result, the composites with MWCNTs as fillers have lower conductivity. On the other hand, CCB has an ability to form a spider-like 3D network structure observed as the circles in Figures 5b and demonstrated in Figure 6b. However, the conductivity of CCB is limited due to their intrinsic feature. Thus, according to Figure 4B, ternary composites might be the best solution to

overcome these individual problems to obtain a complementary effect from MWCNTs and CCB, as shown in Figure 6c. As a result, the ternary composites showed much higher conductivity.

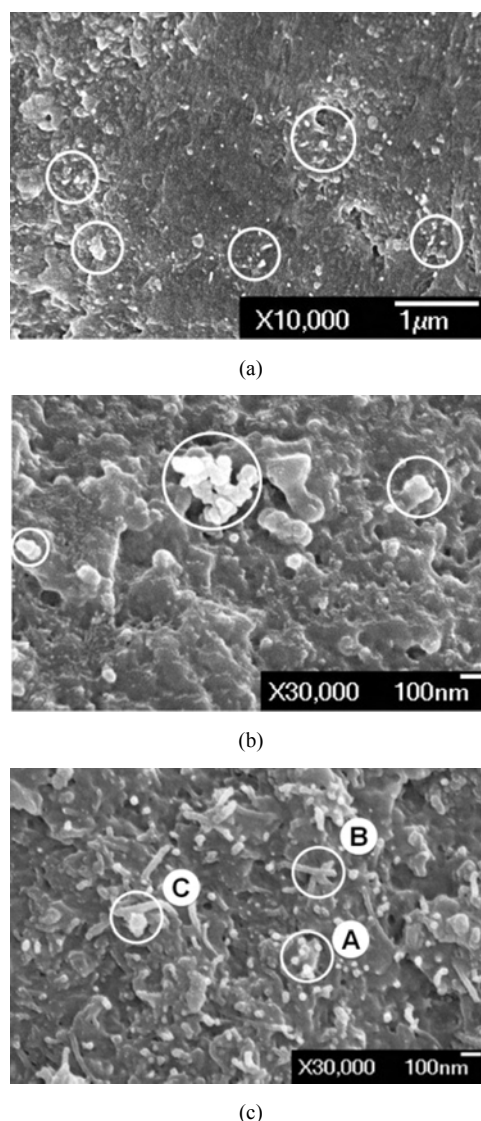
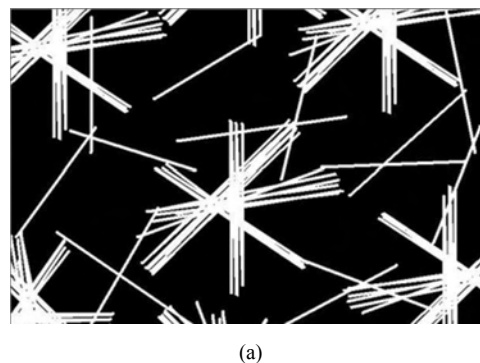


Fig. 5. FESEM micrographs of (a) PN 20, (b) PB 20 and (c) PBN10.



(a)

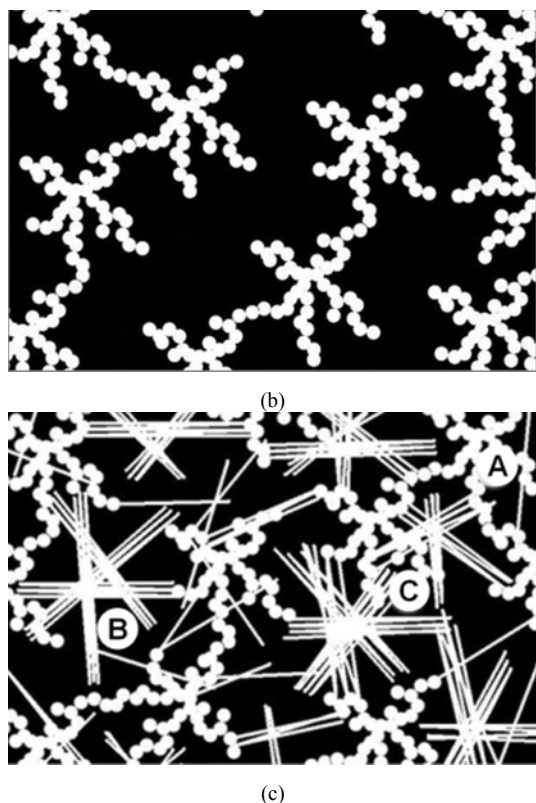


Fig. 6. Schematic diagrams for possible conductive mechanisms of (a) PN composites, (b) PB composites and (c) PBN composites.

4. Conclusions

In this work, a schematic mechanism has been proposed to explain why the properties of the ternary composite system are better than those of the binary systems. Therefore, our formulations will give an innovative idea to potential researchers in the fabrication of other composite systems with superior properties.

Acknowledgements

Authors want to express their sincere gratitude to Timcal Ltd. for providing the CCB used in this work. This work was supported by the A*STAR SERC Grant (0721010018), Singapore.

References

- [1] Wampler WA, Carlson TF, Jones WR, (2003) In *Rubber Compounding – Chemistry and Applications*; Rodgers B, Ed, Marcel Dekker, Inc.: New York, 239-84
- [2] Boonstra BB, (1967) *Journal of Applied Polymer Science*, 11:389-406
- [3] Lee CH, Kim SW, (2000) *Journal of Applied Polymer Science*, 78:2540-6
- [4] Ghofraniha M, Salovey R, (1998) *Polymer Engineering & Science*, 28:58-63
- [5] Lee GJ, Suh KD, Im SS, (1998) *Polymer Engineering & Science*, 38:471-7
- [6] Narkis M, Ram A, Flashner F, (1978) *Polymer Engineering & Science*, 18:649-53
- [7] Tang H, Liu ZY, Piao JH, Chen XF, Lou YX, Li SH, (1994) *Journal of Applied Polymer Science*, 51:1159-64
- [8] Gruenberger TM, Priese A, Van Bellinghen C, Grivei E, Ciallella C, Probst N, (2008) *Plastics & Rubber Singapore Journal*, 15:21-8
- [9] Grunlan JC, Gerberich WW, Francis LF, (2001) *Polymer Engineering & Science*, 41:1947-62
- [10] Kim DJ, Seo KH, Hong KH, Kim SY, (1999) *Polymer Engineering & Science*, 39:500-7
- [11] Koysuren O, Yesil S, Bayram G, (2006) *Journal of Applied Polymer Science*, 102:2520-6
- [12] Iijima S, (1991) *Nature*, 354:56-8
- [13] Lee CJ, Park J, Kang SY, Lee JH, (2000) *Chemical Physics Letters*, 326:175-80
- [14] Saito R, Dresselhaus G, Dresselhaus MS, (1998) *Physical properties of carbon nanotubes*; Imperial College Press: London
- [15] Ebbesen TW, (1996) *Journal of Physics and Chemistry of Solids*, 57:951-5
- [16] Treacy MMJ, Ebbesen TW, Gibson JM, (1996) *Nature*, 381:678-80
- [17] Andrews R, Jacques D, Minot M, Rantell T, (2002) *Macromolecular Materials and Engineering*, 287:395-403
- [18] Yoo HJ, Jung YC, Sahoo NG, Cho JW, (2006) *Journal of Macromolecular Science, Part B Physics*, 45:441-51
- [19] Sahoo NG, Jung YC, Yoo HJ, Cho JW, (2006) *Macromolecular Chemistry and Physics*, 207:1773-80
- [20] So HH, Cho JW, Sahoo NG, (2007) *European Polymer Journal*, 43:3750-6
- [21] Hou H, Ge JJ, Zeng J, Li Q, Reneker DH, Greiner A, Cheng SZD, (2005) *Chemistry of Materials*, 17:967-73.
- [22] Sen R, Zhao B, Perea D, Itkis ME, Hu H, Love J, Bekyarova E, Haddon RC, (2004) *Nano Letters*, 4:459-64.
- [23] Zhang WD, Shen L, Phang IY, Liu T, (2004) *Macromolecules*, 37:256-9
- [24] Lo'pez Manchado MA, Valentini L, Biagiotti J, Kenny JM, (2005) *Carbon*, 43:1499-505
- [25] Safadi B, Andrews R, Grulke EA, (2002) *Journal of Applied Polymer Science* 2002, 84:2660-69
- [26] Jun'ichi M, John MT, (2008) *Macromolecules*, 41:5974-77
- [27] Zhang Q, Fang F, Zhao X, Li Y, Zhu M, Chen D, (2008) *Journal of Physical Chemistry B*, 112:12606-11



<http://www.springer.com/978-1-84996-431-9>

Proceedings of the 36th International MATADOR
Conference

Hinduja, S.; Li, L. (Eds.)

2010, XIX, 598 p. 848 illus., 48 illus. in color. With
CD-ROM., Hardcover

ISBN: 978-1-84996-431-9